MR 66-037

SEMIANNUAL STATUS REPORT NO. 1

INVESTIGATION OF METEOROLOGICAL MEASUREMENT TECHNIQUES UP TO 100 KILOMETERS

First Semiannual Report Under
Grant NGR-45-003-025

For the period
1 October, 1965, through 31 March, 1966

University of Utah
Electrical Engineering Department

Forrest L. Staffanson
Principal Investigator

April 15, 1966

Forrest L. Staffanson
Forrest L. Staffanson

TABLE OF CONTENTS

RESEARCH PERFORMED DURING REPORTING PERIOD

Research has concentrated on the construction of a mathematical model and computer simulation of the flat plate thin substrate type thin film meteorological temperature sensor. Previous work for the Naval Ordnance Laboratory had produced a model neglecting the conduction in the plane of the substrate (Ref. 1, p. 39). During the initial period of this research a supplementary theoretical model was conceived which provides a quantitative indication of this error source, and illustrates the tradeoffs between design parameters. A brief presentation of this is included in Appendix A.

A computer program was derived, programmed, and tested which computes the time-varying temperature distribution in a flat-plate sensor. This integrator allows the specification of the substrate dimensions, boundaries, and composition, including deposited thin film layers of chemically stabilizing, radiation shielding, electrically conducting, or temperature sensing materials. Virtually any conductor configuration on the substrate can be specified in this integrator. The intended general purpose qualities of the integrator cause it to be somewhat expensive in machine time. Research has continued toward decreasing the computer time required in its use. Alternate approaches are under investigation. Appendix B illustrates some of the preliminary results produced by the integrator. A complete thin film sensor simulator is envisioned which may include an improved version of this integrator, together with means of computing or introducing the effects

of parachute motion, radiation and convective environments, electrical currents, and perhaps characteristics of the data handling and processing systems.

Investigation has been under way in response to certain questions which have arisen in connection with the technical activities at NASA Langley Research Center. The notion that immersion thermometers must be larger in dimension than the atmospheric mean free path length is under scrutiny. It appears that there is advantage in decreasing sensor size down to the vicinity of the mean free path length, but neither advantage nor disadvantage in decreasing beyond this limit. Some observations generated during the reporting period are included in Appendix C.

The relative merit with respect to radiation error of different sensor shapes has been under study. Certain data concerning radiation geometric factors for spheres, plates, and cylinders are indicated in Appendix D. Data are yet being gathered concerning the nature (time variation, degree of inhomogeneity, and uncertainty) of the natural radiation environment (albedo and longwave). The null region of the planar sensor (in the plane of the sensor) may prove to be a useful feature of that shape, especially in connection with the radiation shield concept. Analyses anticipating industrial development of prototype hardware using these ideas are being pursued and will be reported as results are obtained. Preliminary thinking on the active shield is indicated in Appendix E.

Previous work on the radar-tracked inflated falling sphere technique (Ref. 2, p. 56) succeeded in detecting and evaluating a cyclic radar error from the radar data. Further work is getting under way toward evaluating radar errors systematically per flight. Appendix F contains preliminary ideas in this direction. Close cooperation from Sandia Corporation in their current inflated falling sphere experiments is expected to provide valuable information and data inputs to this work. It is hoped that sufficient information and data from a variety of other radar-tracked high altitude sphere flights, such as those of the University of Michigan at Wallops and at sea, and perhaps those of P. H. Q. Pearson at Woomera, will be obtained also.

Some time is required during the course of the work, especially in the initial period of the project, to obtain and orient selected graduate research assistants. More such students will join the project in the summer and ensuing academic quarters, and acceleration of the work will follow accordingly. Two master's theses are expected to be completed during the next report period together with publication of the associated research.

Travel included two trips, one during the week of 30 January to 4 February, 1966, with visits to NASA Marshall Space Flight Center, Huntsville, Alabama (Mr. T. C. Bannister on radiation environment), ESSA National Weather Records Center (Dr. H. Crutcher on the error study for Langley), ESSA Office of Meteorological Research (Dr. S. Teweles on instrument error experiments), NASA Langley Research Center (Mr. R. Henry et al., for coordination and technical discussion relative to the project),

and the Naval Ordnance Laboratory (Mr. G. Sloan on Robinette experiments and data processing). The second trip was to the Sixth Conference on Applied Meteorology of the American Meteorological Society with the American Institute of Aeronautics and Astronautics in Los Angeles, 28-31 March, 1966. Professor D. R. Dickson of the University's Meteorological Department and two graduate research assistants also attended this conference in connection with the research activities under the grant. Worthwhile discussions at UCLA (Drs. M. G. Wurtele of Meteorology, C. T. Leondes of Engineering, and others) were held also while in Los Angeles. Technical discussions were held while at this meeting with technical monitoring personnel from NASA Langley Research Center.

REFERENCES

1. Staffanson, F. L., Study of Thin Film Sensors For High Altitude Temperature, Final report under Contract N60921-7156 for the Naval Ordnance Laboratory, White Oak, Silver Spring, Maryland, 15 October 1965.

2. Staffanson, F. L., and Phillips, Kenneth E., Falling Sphere-Radar Mathematical Simulation Techniques, Final Report under NASA grant NGR 45-003-016, September 1965.

APPENDIX A

ON THE CONDUCTION ERROR IN THE THIN SUBSTRATE

A quantitative indication of the thin substrate sensor error due to thermal conduction to the support frame is given by the following one-dimensional model. Consider a thin planar substrate of thickness δ held in a circular frame of radius b. Let the frame temperature T_f, the convective equilibrium temperature T_e (the steady state sensor temperature with zero conduction error), and the effective coefficient of convective heat transfer H all be constant. Let the conductive properties of the substrate be represented by the usual symbols: k, thermal conductivity; ρ, mass density, c, specific heat. The heat equation then is

$$\frac{\partial^2\theta}{\partial r^2} + \frac{1}{r}\frac{\partial\theta}{\partial r} = \frac{\rho c}{k}\frac{\partial\theta}{\partial t} + \frac{2H}{k\delta}\theta$$

$$\theta(b, t) = \theta_f, \quad \left|\theta(0, t)\right| = \text{finite}$$

where r is the radial position in the substrate and $\theta = T - T_r$.

Applying the Laplace transform and imposing the additional boundary condition of uniform initial temperature brings the equation for the transformed variable $\varphi(r, s)$

$$\varphi'' + \frac{1}{r}\varphi' - \left(\lambda^2 + \frac{s}{a^2}\right)\varphi + \frac{\theta_f}{a^2} = 0$$

where we have set $\lambda^2 = \frac{2H}{k\delta}$, $a^2 = \frac{k}{\rho c}$, $\theta(r, 0) = \theta_f$. This is a modified Bessel equation of zero order in the translated variable $\theta(r, s) - \theta_f/\left(s + \lambda^2 a^2\right)$. The linear translation in s indicates a time constant

$$\tau = 1/\lambda^2 a^2 = \rho c \delta / 2H$$

which is identically the principal time constant of the thin substrate, independent of the frame, discussed elsewhere (Staffanson 1965, pp. 44-48) and corresponds to the "first" time constant observed in experiment (Weld, Lunde 1965, pp. 6.1 ff). We have eliminated Weld's "second" time constant here by postulating constant boundary temperatures. The rapid thermal response of the thin substrate, demonstrated both theoretically and experimentally in the cited references, essentially assures continuous thermal equilibrium of the sensor. Therefore the conduction error will be that associated with the steady-state condition.

The steady-state temperature distribution in the present model is given by the time-independent heat equation

$$\theta'' + \frac{1}{r}\theta' - \lambda^2\theta = 0, \quad \theta(b) = \theta_f, \quad \left|\theta(0)\right| = \text{finite}$$

The boundary condition requiring the solution to be finite at the origin necessitates rejection of the modified Bessel function of the second kind, leaving us for the solution the modified Bessel function of zero order of the first kind. Applying the boundary temperature at the frame brings

the solution

$$\theta(r) = \frac{\theta_f}{I_0(\lambda b)} I_0(\lambda r)$$

This temperature distribution is illustrated in Fig. 1.

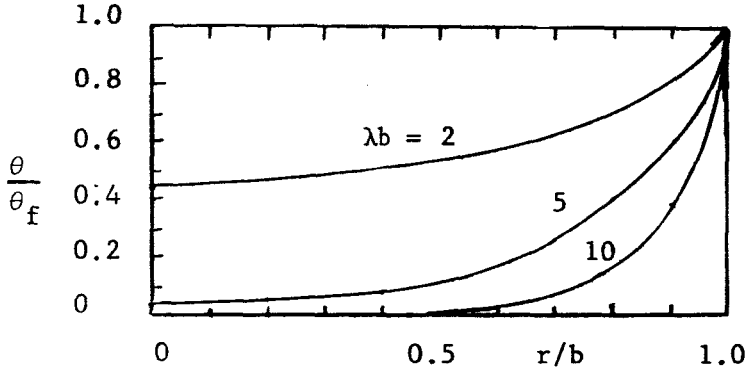

r/b	θ/θ_f (see Ref. 3, Tables 4.4, 9.8)		
	λb = 2	5	10
0.0	0.44	0.0365	
0.2		0.046	
0.4	0.51	0.083	
0.5	0.55		0.0097
0.7			0.06
0.8		0.415	0.152
0.9			0.39

Fig. 1. Steady-state conduction error in a uniform thin substrate.

Several useful parametric curves can be derived from this model according to need. The conduction error would be some average of the

temperature over the sensing region of the substrate. Suppose, for illustration, that the sensing region is centered with radius b/2, and it is desired that the temperature of this sensing region remain within one degree of T_r (i.e., $\theta < 1$), though the frame temperature may exceed T_r by as much as 100 degrees $\left(\theta/\theta_f < 0.01\right)$. Then it is seen from Fig. 1 that the parameter $\lambda b = b\sqrt{\frac{2H}{k\delta}}$ must be about 10 or greater. If, further, this is to be required at 70 km altitude where H is approximately unity for typical fall speeds, and the substrate (frame) is 1 cm in diameter and has thermal conductivity k = 0.03 cal/m sec °k, then its thickness must not exceed about 17 microns or 2/3 mil.

$$\delta = \frac{2Hb^2}{(\lambda b)^2 k} = \frac{2(1.0)(0.005)^2}{10^2(0.03)} = 17 \times 10^{-6}\,m$$

Since substrate thicknesses of considerably less than this are anticipated, it appears that there will be allowance for additional conductive effects of the electrical conductors and ample latitude for adjustment of the various design parameters in arriving at an optimal configuration.

A two-dimensional model which includes the thermal effects of the electrical conductors on the substrate will prove useful for the study of specific sensor designs.

REFERENCES

1. Weld, Samuel A., and Lunde, Kenneth O., "Thin Film Thermister Temperature Sensor," Final Report for Naval Ordnance Laboratory Contract No. N60921-7136, Metro Physics Inc., Santa Barbara, California, 4 September, 1965.

2. Staffanson, Forrest L., "Study of Thin Film Sensor for Naval Ordnance Laboratory," Contract No. N60921-7156, Upper Air Research Laboratory, University of Utah, Salt Lake City, Utah, 15 October, 1965.

3. Abramowitz, Milton, and Stagun, Irene H., "Handbook of Mathematical Functions," National Bureau of Standards AMS 55, June 1964.

APPENDIX B

A RESULT FROM THE PLANAR THIN SUBSTRATE INTEGRATOR, VERSION I

The thermal response of the hypothetical sensor described in Fig. 1 and Table I below was computed by the planar thin substrate

TABLE I

SENSOR CONSTANTS

	Substrate	Conductor
Thickness	6×10^{-6} m	1×10^{-6} m
Thermal conductivity	0.151 watts/m°K	293 watts/m°K
Specific heat	1254 joules/kg°K	128 joules/kg°K
Mass density	1390 kg/m^3	19,300 kg/m^3
Absorptivity	0.2	0.2

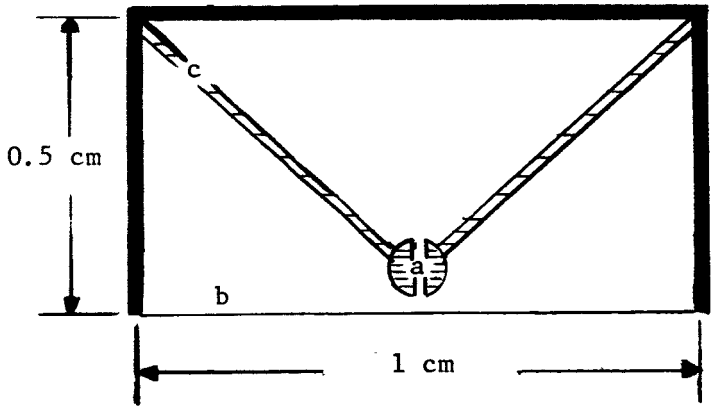

Fig. 1. Conductor configuration.

integrator (version I). The temperature of the U-shaped frame was held constant at the initial uniform value (300°K), while the film temperature T(x, y, t) responded to the convective, conductive and

radiative environment. The environment also was held constant for this run according to nominal conditions for parallel flow at 70 km altitude in daylight shade. The solution was produced at 40^{-1}cm intervals over the film. Fig. 2 illustrates the behavior in time of selected points

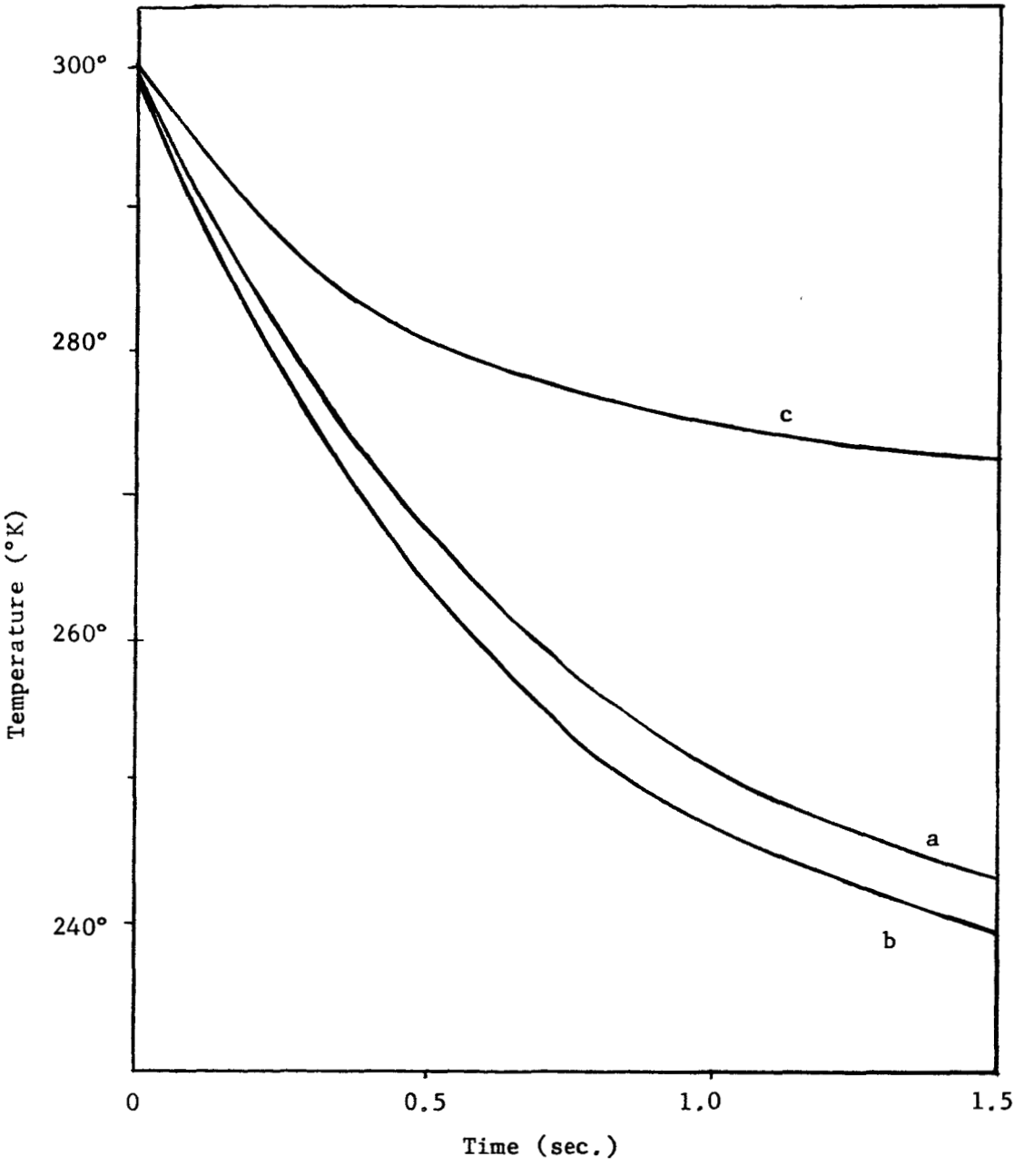

Fig. 2. Time history at selected points on the sensor.

on the film. Point "a" represents the position of the temperature sensing element. Point "b" represents a point remote from the conductor, and point "c" is on the conductor film about one-eighth of the distance from the frame to the sensitive point "a." The integrator output is illustrated by the temperature distribution at t = 1.5 sec. tabulated in Table II.

Since the hypothetical model is symmetric with respect to the center line, only the temperature distribution of the left half plane was computed.

TABLE II

SENSOR TEMPERATURE DISTRIBUTION AT 1.5 SECONDS

300.0	300.0	300.0	300.0	300.0	300.0	300.0	300.0	300.0	300.0	300.0
300.0	295.1	290.6	277.4	267.6	263.0	261.0	260.3	259.9	259.8	259.8
300.0	279.9	286.3	282.3	267.0	254.9	249.5	247.3	246.4	246.1	246.0
300.0	268.6	269.3	278.6	275.2	260.9	249.5	244.6	242.6	241.8	241.5
300.0	263.5	255.8	262.9	272.1	269.3	256.9	246.9	242.7	241.0	240.3
300.0	261.2	249.9	250.3	258.5	266.7	264.4	253.8	245.4	241.8	240.4
300.0	260.3	247.5	244.9	247.5	255.2	262.2	260.3	251.4	244.3	241.4
300.0	250.0	246.5	242.7	242.9	245.9	252.5	258.5	256.9	249.5	243.5
300.0	259.8	246.1	241.8	241.1	242.1	244.8	250.4	255.4	254.1	247.9
300.0	259.8	246.0	241.5	240.4	240.5	241.5	243.9	248.6	252.8	251.7
300.0	259.8	246.0	241.4	240.1	239.9	240.2	241.2	243.2	247.2	250.7
300.0	259.8	245.9	241.4	240.0	239.7	239.8	240.1	240.9	242.6	246.0
300.0	259.8	245.9	241.4	240.0	239.6	239.6	239.7	240.0	240.7	242.1
300.0	259.8	245.9	241.4	240.0	239.6	239.5	239.5	239.6	239.9	240.5
300.0	259.8	245.9	241.4	240.0	239.6	239.5	239.5	239.5	239.6	239.9
300.0	259.8	245.9	241.4	240.0	239.6	239.5	239.5	239.5	239.5	239.6
300.0	259.8	245.9	241.4	240.0	239.6	239.5	239.5	239.5	239.5	239.5
300.0	259.8	245.9	241.4	240.0	239.6	239.5	239.5	239.5	239.5	239.5
300.0	259.8	245.9	241.4	240.0	239.6	239.5	239.5	239.5	239.5	239.5
300.0	259.8	245.9	241.4	240.0	239.6	239.5	239.5	239.5	239.5	239.5
300.0	259.8	245.9	241.4	240.0	239.6	239.5	239.5	239.5	239.5	239.5

Table II, continued

300.0	300.0	300.0	300.0	300.0	300.0	300.0	300.0	300.0	300.0
259.8	259.8	259.8	259.8	259.8	259.8	259.8	259.8	259.8	259.8
246.0	245.9	245.9	245.9	245.9	245.9	245.9	245.9	245.9	245.9
241.4	241.4	241.4	241.4	241.4	241.4	241.4	241.4	241.4	241.4
240.1	240.0	240.0	240.0	240.0	240.0	240.0	240.0	240.0	240.0
239.9	239.7	239.6	239.6	239.6	239.6	239.6	239.6	239.6	239.6
240.2	239.7	239.6	239.5	239.5	239.5	239.5	239.5	239.5	239.5
241.0	240.1	239.7	239.5	239.5	239.5	239.5	239.5	239.5	239.5
242.9	240.8	240.0	239.6	239.5	239.5	239.5	239.5	239.6	239.6
246.5	242.4	240.6	239.9	239.6	239.6	239.6	239.7	239.8	240.0
249.8	245.5	241.9	240.5	239.9	239.8	239.9	240.2	240.6	241.3
249.0	248.2	244.6	24.16	240.5	240.3	240.6	241.6	242.3	243.6
245.0	247.5	246.9	243.9	241.6	241.1	242.3	243.7	243.7	243.7
241.8	244.2	246.3	245.8	243.4	242.4	243.7	243.7	243.7	243.7
240.4	241.4	243.5	245.3	244.9	243.4	243.8	243.8	243.7	243.7
239.9	240.3	241.2	243.0	244.5	244.1	243.9	243.8	243.8	243.7
239.6	239.8	240.2	241.0	242.5	244.0	243.9	243.8	243.8	243.7
239.5	239.6	239.8	240.1	240.9	242.3	243.8	243.8	243.7	243.7
239.5	239.5	239.6	239.7	240.1	240.8	242.3	243.7	243.7	243.7
239.5	239.5	239.5	239.6	239.7	240.0	240.7	241.7	242.4	243.7
239.5	239.5	239.5	239.5	239.8	239.7	240.0	240.5	241.0	241.7

APPENDIX C

ON THE MINIMAL SIZE OF ROCKETSONDE TEMPERATURE SENSORS

The notion that there is a minimal characteristic length for optimal performance of a parachute-borne high-altitude immersion-type meteorological temperature sensor is examined in the following way.

Consider the heat equation of the sensor (the body located in the air stream) in the simple form

$$C \frac{\partial T}{\partial t} = hA \left(T_r - T \right) + q$$

where

T = sensor temperature (considered uniform for small sensors)

C = sensor heat capacity

t = time

h = convective coefficient

A = sensor (convective) surface area

T_r = recovery temperature of the air stream relative to the sensor

q = heat input rate to the sensor due to all sources other than convection (i.e., all sources of sensor error)

If C (or the sensor time constant) is sufficiently small, the dynamic error will be insignificant and T will continuously follow its equilibrium value.

$$T_e = T_r + \frac{(q/A)}{h}$$

The sensor steady-state error deriving from heat sources other than convective heat transfer with the air stream, including

a. Radiation with the local and distant environment

b. Electric power dissipation within the sensor due to radio-frequency or monitoring currents

c. Thermal conduction through supporting or electrical connections

is given by q/hA. Since the most formidable among these error sources for future designs will likely be radiation, and since radiative heat input is in general proportional to A, we assert that q/A for a given sensor configuration is essentially independent of sensor size. Thus the dependence of the sensor error on characteristic length resides in h.

We are lead to ask how h depends on size, i.e., to examine the function h(L), where L is the characteristic length of the sensor. Choosing the flat plate in parallel flow, and the flow conditions associated with the altitude interval $60 \leq z \leq 90$ km, we find that the flow regimes encountered extend from the free molecule to slip flow. Associated parameter values are tabulated in Table I [Staffanson, 1965]. L_t and L_c are the characteristic lengths associated with the transition flow boundary $\left(M/\sqrt{R_e} = 0.1\right)$ and the continuum flow boundary $\left(M/\sqrt{R_e} = 0.01\right)$ respectively. The atmospheric parameters are taken from the U. S. Standard Atmosphere 1962. The remaining quantities are based on approximate ARCAS parachute fall speeds, except that an arbitrary fall speed of 440 m/s was used at 90 km.

The convection coefficient is available for free-molecule flow from Oppenheim (1953) in terms of Stanton number S_t and accommodation coefficient α (to which we shall assign the arbitrary value $\alpha = 0.88$

TABLE I

PARAMETER VALUES ASSOCIATED WITH FLOW CONDITIONS ON A TYPICAL METEOROLOGICAL SONDE

z(km)	60	70	80	90
$\rho\left(kg/m^3\right)10^5$	30.6	8.75	2.00	.317
V(m/sec)	93	174	367	440
V_s(m/sec)	321	297	269	269
M	.29	.54	1.36	1.63
$\eta\left(m^2/sec\right)$	.0532	.164	.609	3.84
R_e	1750L	1060L	604L	115L
$L_t(m)10^3$	.0048	.0326	.292	2.32
L_c(m)	.48	3.26	29.2	232
$k(watt/m°K)10^3$	22.7	19.8	17.4	16.4
$\lambda(m)10^{-3}$	0.266	.928	4.07	25.6

for plotting purposes).

$$h = \alpha\left(\frac{S_t}{\alpha}\right)V\rho C_p \qquad L \ll \lambda$$

In free-molecule flow h is independent of L, though $L > 10\lambda$ will indicate transition or slip flow conditions rather than free molecule conditions.

Under slip-flow conditions S_t is taken from the expression [Drake and Kane 1950]

$$S_t = \frac{0.38}{MX_2^2}\left[\exp\left(X_2^2\right)\operatorname{erfc}\ X_2 - 1 + \frac{2}{\sqrt{\pi}}X_2\right],\quad 0.01 < \frac{M}{\sqrt{R_e}} < 0.1$$

$$X_2 = \sqrt{\frac{R_e P_r}{6.9M^2}}$$

The dependence of the convection coefficient on the sensor size h(L), according to the above considerations, is displayed by Fig. 1. Expressions for the transition regime are notably absent. It has been the practice of the author and others to assume a simple interpolation between the free molecule and the bordering slip-flow values for convection coefficient values in the transition region. Unless additional information exists indicating a significantly larger h than is indicated by the interpolated curves (such as might be provided by empirical agreement with extrapolation of the slip-flow function beyond its published limit), there is no reason to expect a decrease in meteorological sensor performance when its size decreases beyond the mean free path. There appears to be an advantage in decreasing sensor size down to the size at which the flow enters the transition region, and perhaps a decreasing advantage down to the vicinity of the mean free path length. Smaller sizes would be expected to demonstrate no increased (nor decreased) accuracy with respect to radiation errors. Notice that the advantage of decreasing a given sensor size is realized more at the lower altitudes.

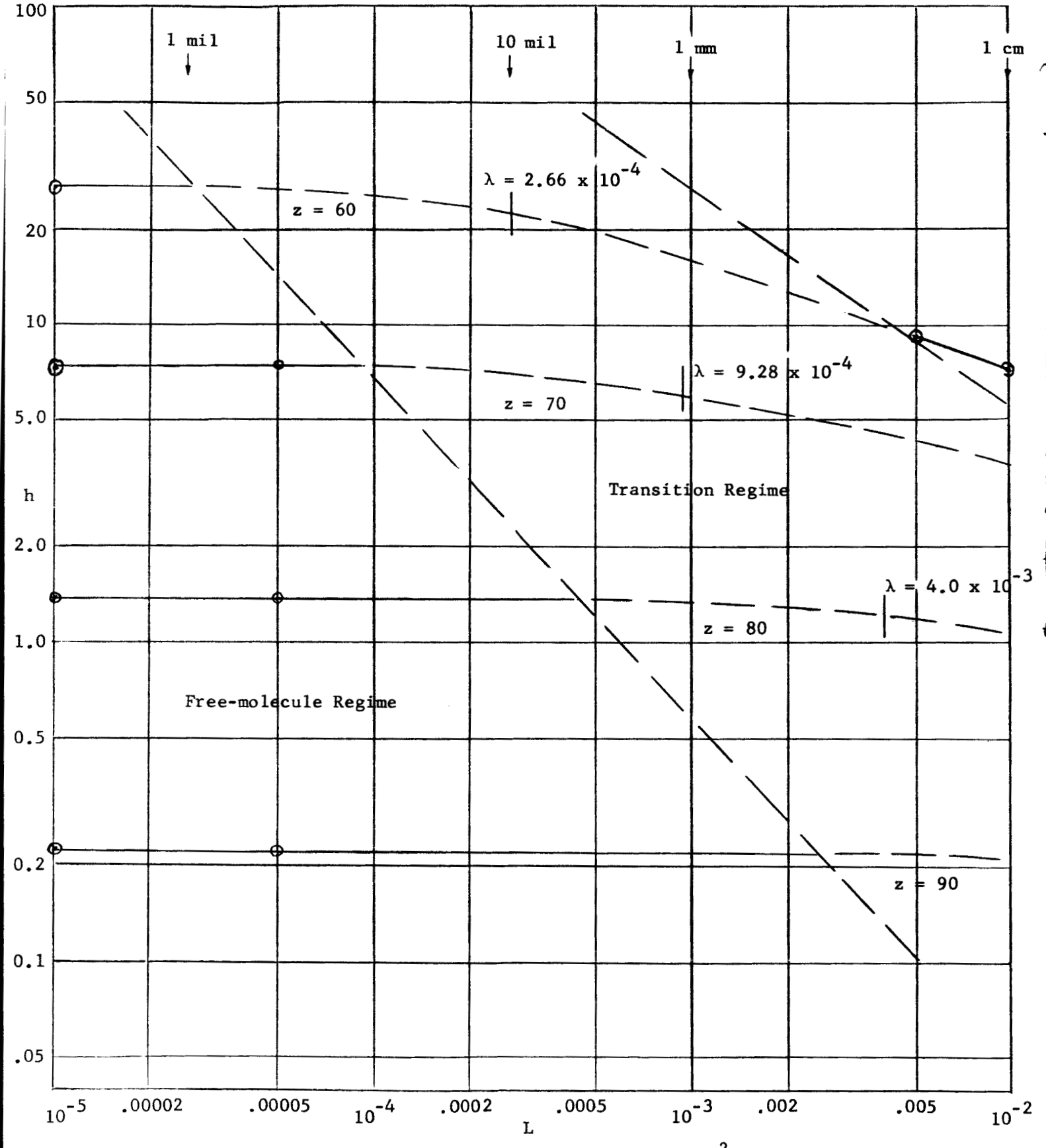

Fig. 1. Flat plate convection coefficient h (watts/°km^2) vs. characteristic length L (meters) at selected altitudes Z (km).

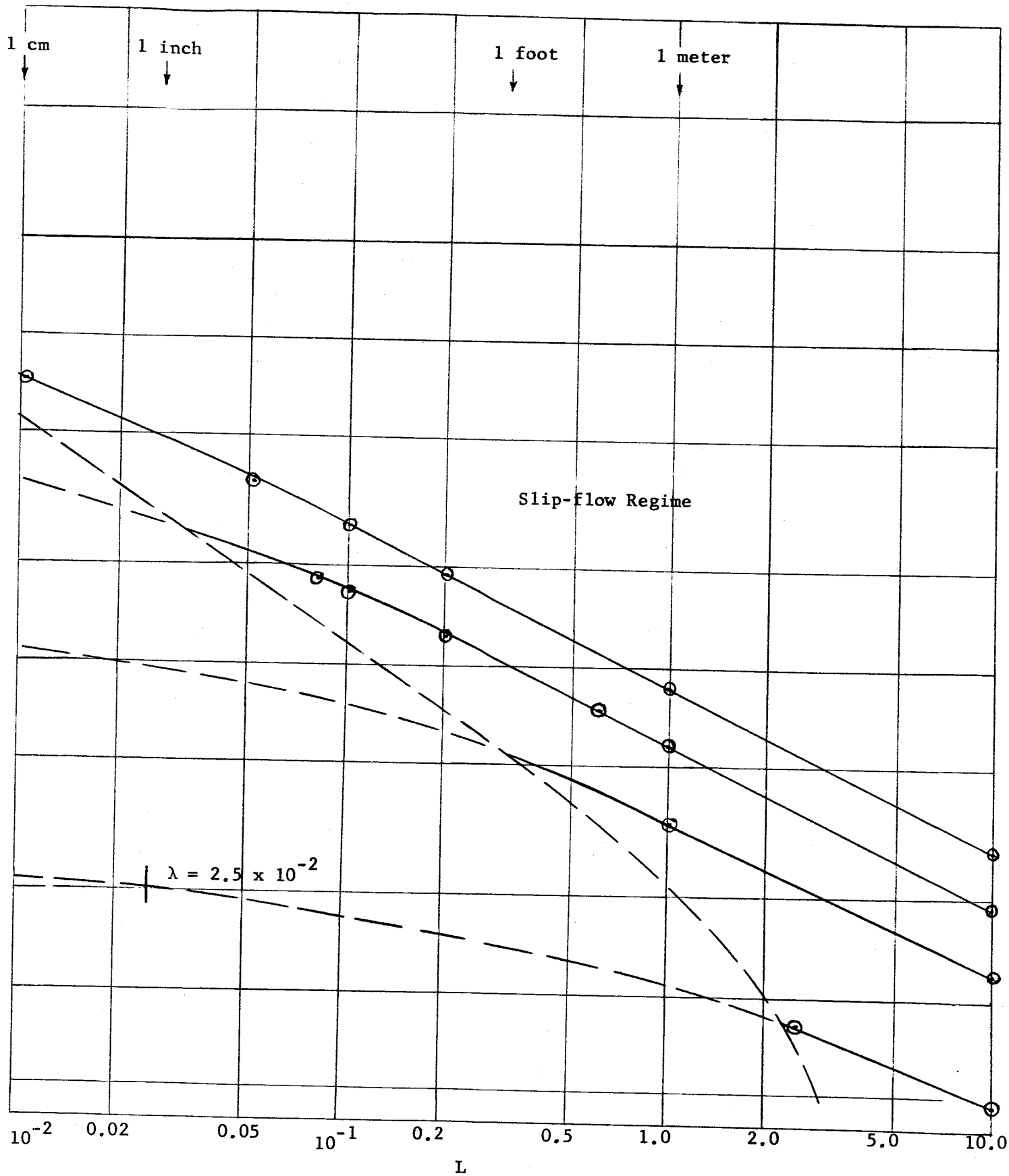

Fig. 1, continued.

These results apply to spheres and cylinders as well as to the flat plate, as illustrated by the following. Consider the average slip-flow expression for spheres [Kavanau 1953, 1955]

$$\bar{N}_u = \frac{N\mathring{u}}{1 + 3.42 \frac{M}{RePr} N\mathring{u}} = \frac{1}{\frac{1}{N^\circ} + \left(3.42 \frac{\eta}{V_s Pr}\right)\frac{1}{D}}$$

where [Eckert and Drake 1959, p. 250]

$$N\mathring{u} = 2 + 0.37\, Re^{0.6} \sqrt[3]{Pr} = 2 + \left[0.37 \sqrt[3]{Pr} \left(\frac{V}{\eta}\right)^{0.6}\right] D^{0.6}$$

The convection coefficient h is given by

$$h = \bar{N}u \frac{k}{D}$$

and for constant flow conditions h(D) is given by

$$h = \frac{k/D}{\frac{1}{N\mathring{u}} + \frac{a}{D}} = \frac{k}{\frac{D}{2 + bD^{0.6}} + a} = k \frac{2 + bD^{0.6}}{D + a\left(2 + bD^{0.6}\right)}$$

The slope of h(D) is seen to be negative as in the case of the flat plate

$$\frac{\partial h}{\partial D} = - \frac{k\left(2 + 0.4bD^{0.6}\right)}{\left[D + a\left(2 + bD^{0.6}\right)\right]^2} < 0$$

and the value of h at the transition boundary is definitely less than that for free molecule flow. Values are listed in Table II.

TABLE II

CONVECTION COEFFICIENTS BORDERING TRANSITION REGION FOR SPHERE

Z(km)	(h slip) max	h molec.
60	9.93	27.5
70	2.15	7.87
80	.4119	1.91
90	.0605	0.334

The diameter associated with the boundary between slip and transition flow is given by the condition $\left(M/\sqrt{R_e}\right) < 0.1$ and is equal to L_t:

$$\frac{M}{\sqrt{R_e}} = \frac{V/V_s}{\sqrt{V\ D_t/\eta}} = 0.1$$

$$D_t = \frac{100}{V_s} M\eta$$

A similar examination for the cylinder brings similar results.

Ney, Maas, and Hugh [1961] state that the heat transfer per unit length per unit temperature difference is a constant, almost independent of the diameter of the cylinder. This implies that the convection coefficient is approximately inversely proportional to the diameter, thus having a negative slope as shown above for the flat plate and sphere. Though the conclusions concerning reduction of sensor size are consistent with the above observations, it is noted

that the study by Ney, et al., concerns balloon-borne sensors and therefore lies in the realm of much lower ventilating speeds (lower than 5 meters/second) and lower altitudes (lower than 50 km, 1mb).

REFERENCES

1. Eckert, E. R. G., and Drake, Robert M., Jr., Heat and Mass Transfer, McGraw-Hill Book Company, Inc., New York, 1959.

2. Kavanau, L. L., "Heat Transfer from Spheres to a Rarefied Gase in Subsonic Flow," Trans. Amer. Soc. Mech. Engineers, Vol. 27, 1955, pp. 617-624.

3. Kavanau, L. L., and Drake, R. M., "Heat Transfer from Spheres to a Rarefied Gas in Subsonic Flow," University of California Report HE 105-108, January 1953.

4. Oppenheim, A. K., "Generalized Theory of Convective Heat Transfer in Free Molecule Flow," J. Aeronaut. Sci., Vol. 20, 1953, pp. 49-48.

5. Staffanson, F. L., "Study of Thin Film Sensors for High Altitude Temperature," Final Report, Contract N60921-7156 for Naval Ordnance Laboratory, White Oak, Silver Spring, Maryland, 15 October, 1965.

6. Drake, R. M., and Kane, E. D., "A Summary of the Present Status of Heat Transfer in Rarefied Gases," University of California Inst. Eng. Research Report HE-150-73, October 1950.

7. Schaaf, S. A., and Chambre, P. L., Flow of Rarefied Gases, Princeton University Press, Princeton, New Jersey, 1961.

8. Ney, Edward P., Maas, Raymond W., and Huch, William F., "The Measurement of Atmospheric Temperature," J. Meteor. 18 February 1961, pp. 60-80.

APPENDIX D

ON THE RELATIVE RADIATION SUSCEPTIBILITY OF THE FLAT PLATE, CYLINDER, AND SPHERE

The radiation incident from a "black" polar cap of temperature T is $\sigma T^4 fA$, where f is a dimensionless geometric factor referred to the area A. Choose A to be the surface area of the small

a. Thin plate, $\pi\rho^2$

b. Short cylinder, $2\pi\rho\ell$

c. Sphere, $4\pi\rho^2$

The geometric factor varies with the magnitude of the solid angle, i.e., half-angle θ_0, subtended by the distant polar cap, and varies with the orientation, i.e., aspect angle γ. Exact analytical functions are derivable for certain specific cases. For example, for the sphere which is symmetric in γ:

$$f = \left(1 - \cos \theta_0\right)/2$$

and for the plate at $\gamma = \pi/2$ (Ref. 1, p.24):

$$f = \frac{\theta_0}{\pi} - \frac{\sin 2\,\theta_0}{2}$$

In cases where every point of each surface sees every point of the other surface, the geometric factor is calculable using Stokes' theorem and a contour integral (Ref. 1). In general, however, numerical integration is required. Data have been adapted from work done elsewhere (Ref. 3) and are exemplified by the Figs. 1, 2, and 3.

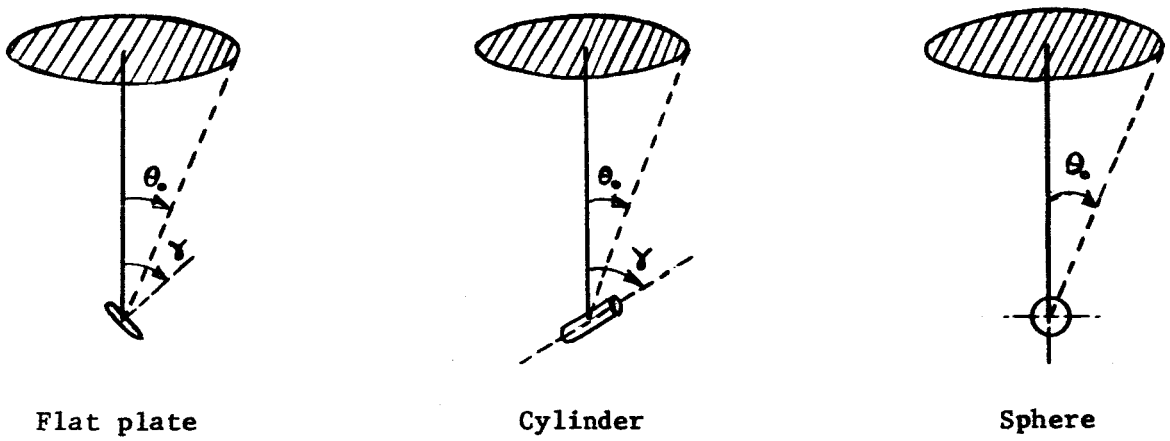

Fig. 1. Illustration of the half angle θ_0 and aspect angle γ.

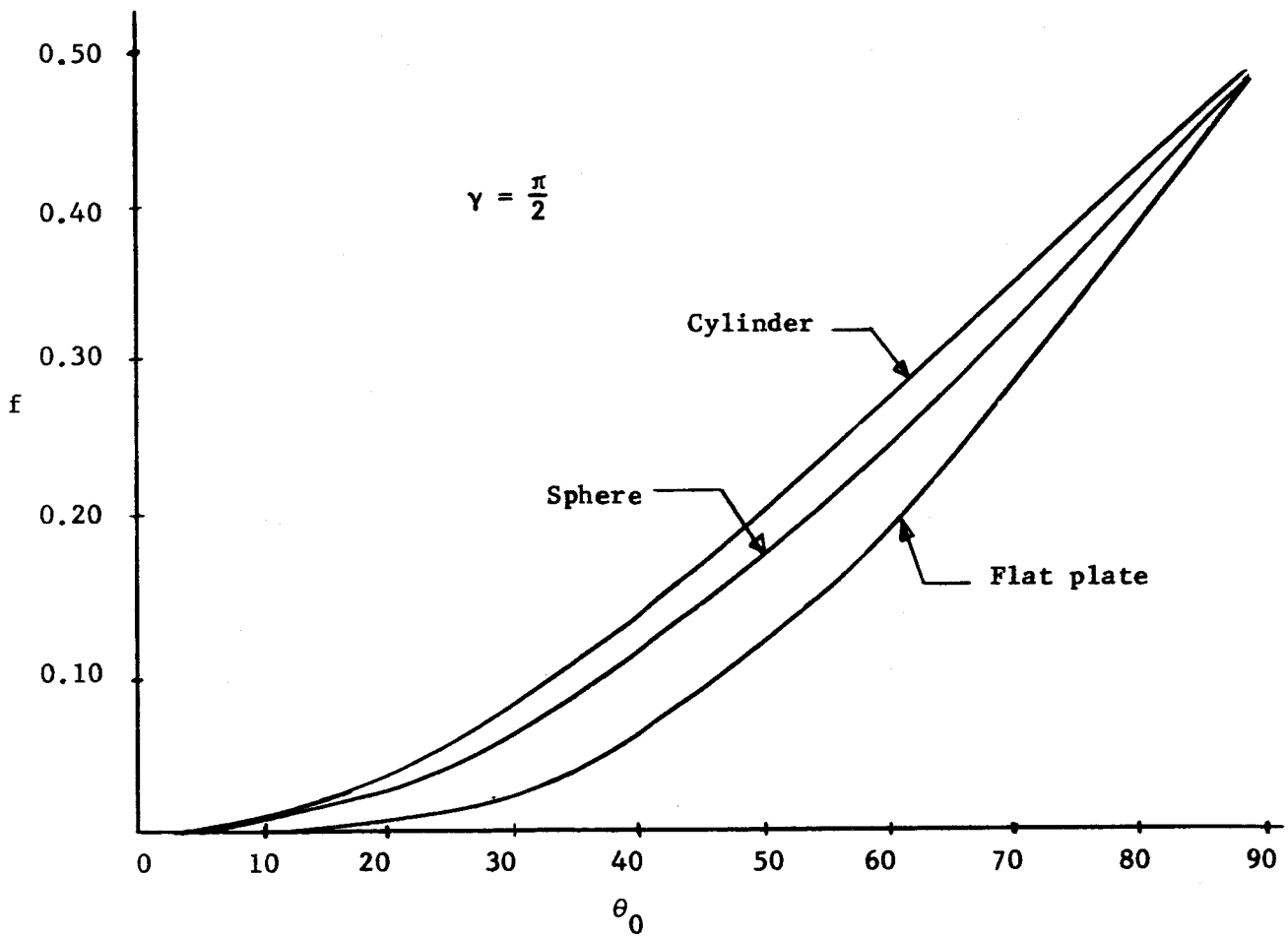

Fig. 2. Comparison of the geometric factor for the flat plate, cylinder, and sphere.

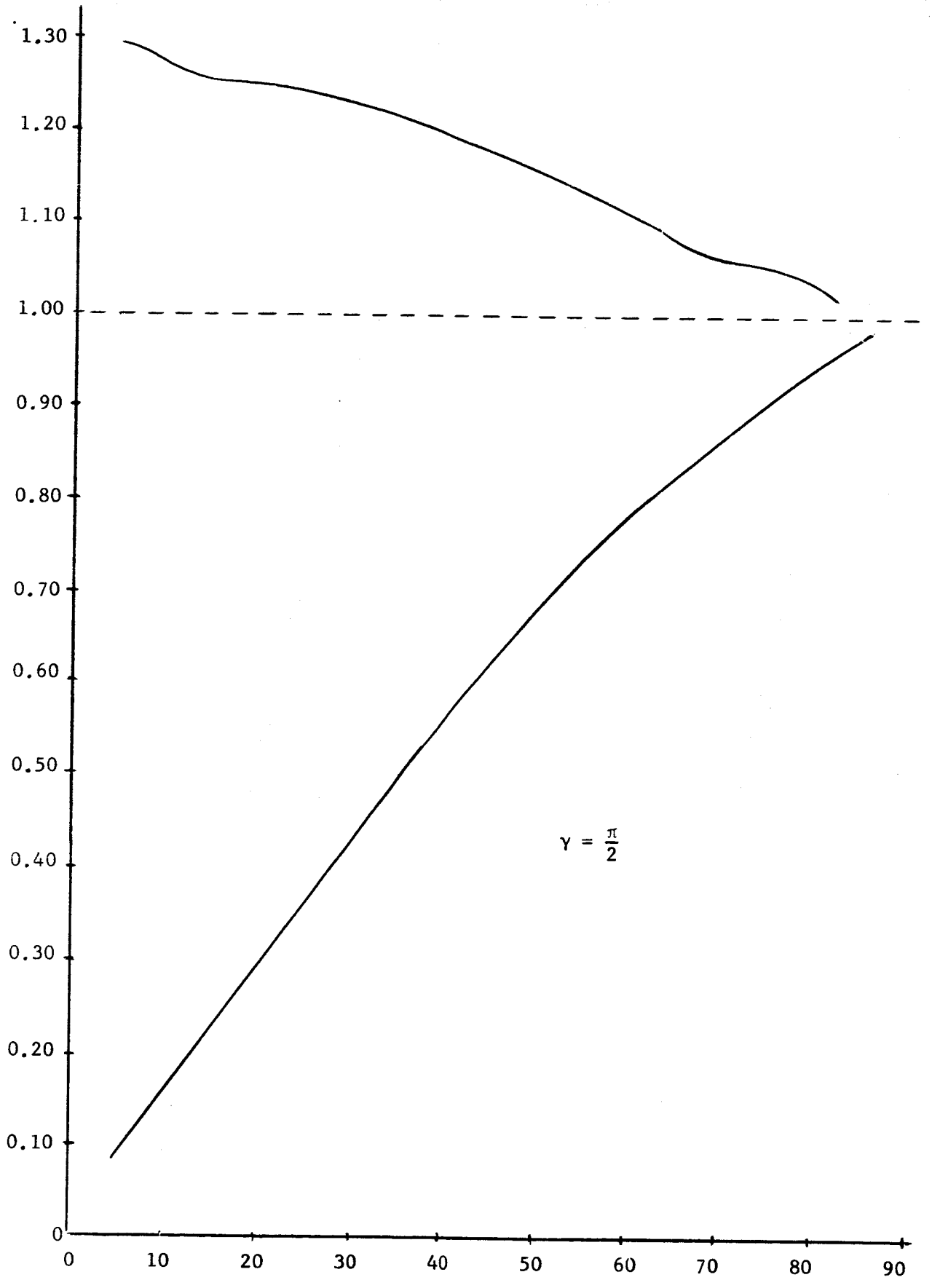

Fig. 3. Geometric factor of the flat plate and cylinder referred to that of the sphere.

The relative radiation susceptibility of given sensor shapes depends on the respective convection coefficients h as well as on the radiation geometric factor f. At equilibrium, assuming no other significant heat inputs, the net heat flow from convection and radiation is zero.

$$hA\left(T_r - T_e\right) + \sigma\, fA\left(T_R^4 - T_e^4\right) = 0$$

Linearizing the quartic terms and solving for the radiation error per degree radiation temperature

$$\frac{T_e - T_r}{T_R - T_r} = \frac{1}{1 + h/\left(4\sigma T_a^3\right)f}$$

the radiation susceptibility may be viewed as a reciprocal function of the ratio h/f scaled according to the nominal temperature T_a and translated by unity.

REFERENCES

1. Staffanson, F. L., "Study of Thin Film Sensors for High Altitude Temperatures," Final Report under Contract N60921-7156 for the Naval Ordnance Laboratory, White Oak, Silver Spring, Maryland, 15 October, 1965.

2. Sparrow, E. M., "A New and Simpler Formulation for Radiative Angle Factors," ASME 85, Series C., No. 2, May 1963, p. 81.

3. Ballinger, J. C., Elizalde, J. C., Gardia-Varela, R. M., and Christensen, E. H., "Environmental Control Study of Space Vehicles, Part II," Thermal Environment of Space, General Dynamics, Convair Division Report ERR-AN-016 Aerophysics, 1 November 1960, with Supplement A, 10 January 1961, and Supplement B, 20 January 1961.

APPENDIX E

COMMENTS ON THE ACTIVE RADIATION SHIELD CONCEPT
FOR METEOROLOGICAL TEMPERATURE SENSORS

Consider a temperature-controlled shield [Billings, 1966] designed to develop a parachute-borne thermometer in such a way as to occlude external thermal radiation, but to admit air for the thermal ventilation of the thermometer sensor. A duct of some kind is therefore implied through which the ventilating air must pass. Equations may be developed as follows for the purpose of investigating the performance of such a thermometer system.

The temperature of the sensor is determined by convective heat transfer with the air inside the duct (i.e., by heat transfer according to combined convective heat transport and thermal conduction in the air near the sensor surface), by radiative heat transfer with the duct walls, by conductive heat transfer with the sensor supporting structure, and by ohmic heating within the sensor.

$$(CA)\frac{dT}{dt} = hA\left(T_f - T\right) + \sigma A_r\left(\epsilon T_s^4 - \alpha T^4\right) + K\left(T_s - T\right) + \beta$$

Linearizing the quartic variables

$$T^4 = aT + b, \quad a = 4T_a^3, \quad b = -3T_a^4, \quad T_a \approx T$$

Letting $A_r = A$ (see Glossary) (the factor A_r/A may be included in σ),

and dividing by this area produces

$$C\dot{T} = h\left(T_f - T\right) + \sigma\left[\epsilon\left(a_s T_s + b_s\right) - \alpha\left(aT + b\right)\right] + \frac{K}{A}\left(T_s - T\right) + \frac{W}{A}$$

$$= -\left(h + \sigma\alpha a + \frac{K}{A}\right)T + hT_f + \left(\sigma\epsilon a_s + \frac{K}{A}\right)T_s + \sigma\left(\epsilon b_s - \alpha b\right) + \frac{W}{A}$$

$$= \Sigma$$

Notice the sensor time constant T_s = constant is

$$\tau = C/(h + \sigma\alpha a + K/A)$$

In order to shield the sensor against radiation from the direction of the incoming air, it would seem necessary to deflect the ventilating air around a corner.* It is suppose that, since the air which reaches the sensor must be deflected by the shield (duct), the sensor will lie within the thermal boundary layer in the duct. Thus the air temperature will be changed accordingly. Under incompressible flow conditions and the gross assumption that the temperature rise in the vicinity of the sensor is some average of that across the duct, the increase of

---

* Possibly the null region of a directional sensor, such as the flat plate, could be oriented toward an inlet aperture, thus admitting "fresh" air with minimal radiation error. A degree of compromise in this way may profitably reduce G and the uncertainity in r' discussed below, and lead to an optimal configuration.

enthalpy due to heat transfer with the duct is

$$C_p \left(T'_\infty - T_\infty\right) = h_s A_s \left(T_s - T_{rs}\right)/\dot{m}$$

So the temperature of the air approaching the sensor is

$$T'_\infty = T_\infty + G\left(T_s - T_{rs}\right)$$

$$G = \frac{h_s A_s}{\dot{m} C_p} = \left(\frac{A_s}{\dot{m}/\rho V}\right)\left(\frac{h_s}{\rho V C_p}\right) = \lambda S_t$$

The recovery temperature of the sensor will depend on a recovery factor associated with the sensor and on the velocity of flow at the sensor.

$$T_f = T'_\infty + r \frac{V_f^2}{2C_p} = T_\infty + G\left[T_s - T_\infty - r_s \frac{V^2}{2C_p} + r \frac{V^2}{2C_p}\right]$$

$$= (1 - G)\, T_\infty + G T_s + r' \frac{V^2}{2C_p}$$

$$r' = r\left(\frac{V_f}{V}\right)^2 - G r_s$$

Notice that in order for the sensor to be responsive to the ambient air temperature, the duct must be designed such that

$$G < 1$$

Reynolds' number at mesospheric heights is of the order of

$$Re = \frac{\rho V L}{\mu} \approx \frac{(10^{-4})(10^{2})(10^{-2})}{10^{-5}} = 10$$

Extrapolating from data presented in Industrial and Engineering Chemistry, Vol. 28, December, 1936, p. 1429 (see Kreith, p. 361), Stanton's number would seem to be of the order of

$$S_t \approx 0.1$$

Thus it would further appear that the duct "length" should be such that

$$\lambda \approx 1$$

Valid evaluation of the parameters G and r' will require detailed analysis of the flow and boundary layer for specific duct shapes and sizes. Since relatively little is known concerning transition flow in "short tubes" [Carley and Smetana 1966], specially designed experiments may be necessary in order to verify or establish ultimately reliable values. This is especially apparent due to the enhanced entrance effects associated with a corner or baffle. Indeed, achieving acceptable values and accuracies for G and r' may well be the central problem of the active shield concept.

Suppose now that the shield temperature is linearly controlled by a servo system which supplies g watts per degree temperature difference

between the sensor and shield.* The shield, of course, receives heat from its environment according to the approximate linearized expression $g_o(T_{oe} - T_s)$, where T_{oe} is the temperature of the shield when it is at equilibrium with its environment. The thermal environment of the shield includes radiation and convection inside as well as outside, and includes conductive paths to the sonde body. Solution of the heat equation for the shield will provide values for g_o and T_{oe}, Thus the heat equation for the shield is

$$C_s \dot{T}_s = g(T - T_s) + g_o(T_{oe} - T_s)$$

$$= -(g + g_o)\, T_s + gT + g_o T_{oe}$$

$$= \Sigma_s$$

Notice the time constant of the shield is $\tau_s = C_s/(g + g_o)$. For finite servo gain g, the equilibrium shield temperature "error" is

$$T_s - T = \frac{g_o}{g + g_o}\,(T_{oe} - T) = \frac{1}{\beta + 1}(T_{oe} - T)$$

$$\beta = g/g_o$$

Notice sufficiently high β will render g_o and T_{oe} insignificant.

---

* An "on-off" or other nonlinear control may prove to be more practical eventually, but the linear assumption is applied for initial modeling.

The nodal equations for the system may be written, in the frequency domain

$$T = \Sigma/CS$$

$$\Sigma = -\left(h + \alpha\alpha a + \frac{K}{A}\right) T + hT_f + \left(\sigma\epsilon a_s + \frac{K}{A}\right) T_s + \sigma\left(\epsilon b_s - \alpha b\right) + \frac{W}{A}$$

$$T_f = GT_s + (1 - G)\, T_\infty + \frac{r'V^2}{2C_p}$$

$$T_s = \Sigma_s/C_sS$$

$$\Sigma_s = gT - \left(g + g_o\right) T_s + g_oT_{oe}$$

The signal-flow diagram may be drawn as follows:

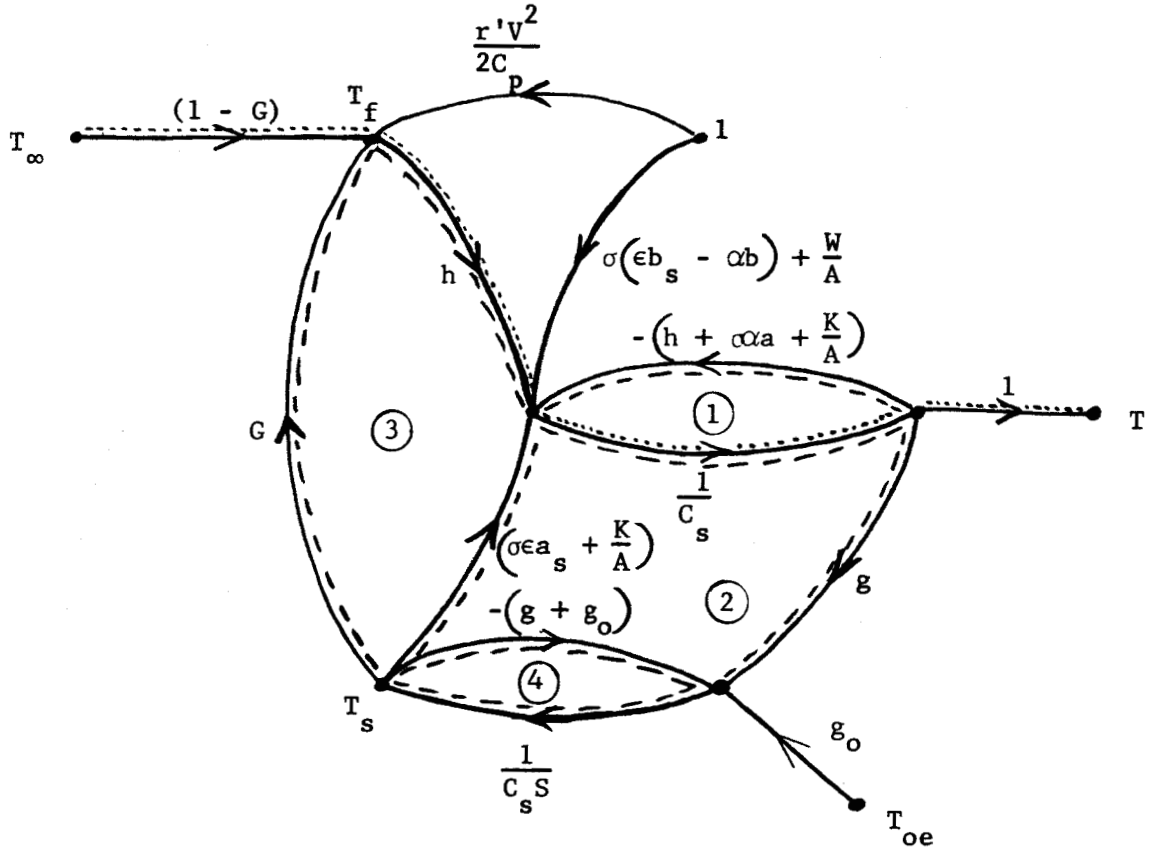

Fig. 1. Signal-flow diagram.

The gain between the sink T (thermometer output) and each of the three sources of the diagram is obtained using Mason's method [Mason, 1953, 1956] and, by superposition, the over-all output function is found to be

$$T(s) = \frac{1}{D}\left\{ \frac{(1 - G)h}{C}\left[S + \frac{g + g_o}{C_s}\right] T_\infty(S) + \frac{g_o\left(Gh + \sigma\epsilon a_s + \frac{K}{A}\right)}{CC_s} T_{oe}(S) + \left[\frac{\sigma\left(\epsilon b_s - \alpha b\right) + \frac{W}{A}}{C} + \frac{hr'V^2}{2C_pC}\right]\left[S + \frac{g + g_o}{C_s}\right]\right\}$$

where the denominator is

$$D = S^2 + \left[\frac{h + \alpha\alpha a + \frac{K}{A}}{C} + \frac{g + g_o}{C_s}\right] S + \frac{g}{CC_s}\left[(1 - G)h + \sigma\left(\alpha a - \epsilon a_s\right)\right] + \frac{g_o}{CC_s}\left[h + \alpha\alpha a + \frac{K}{A}\right]$$

The sensor will seek its equilibrium values ($S = j\omega \rightarrow 0$)

$$T_e = \frac{(1 - G)h\left(g + g_o\right)T_\infty + g_o\left(Gh + \sigma\epsilon a_s + \frac{K}{A}\right)T_{oe} + \left[\sigma\left(\epsilon b_s - \alpha b\right) + \frac{W}{A} + \frac{hr'V^2}{2C_p}\right]\left(g + g_o\right)}{g_o\left(h + \alpha\alpha a + \frac{K}{A}\right) + g\left[(1 - G)h + \sigma\left(\alpha a - \epsilon a_s\right)\right]}$$

which for $g \rightarrow \infty$ becomes

$$\frac{(1 - G)hT_\infty + \sigma\left(\epsilon b_s - \alpha b\right) + \frac{W}{A} + \frac{hr'V^2}{2C_p}}{(1 - G)h + \sigma\left(\alpha a - \epsilon a_s\right)} = \frac{(1 - G)hT_\infty + \sigma b(\epsilon - \alpha) + \frac{W}{A} + \frac{hr'V^2}{2C_p}}{(1 - G)h - \delta a(\epsilon - \alpha)}$$

giving an error

$$T_e - T_\infty = \frac{\sigma(\epsilon - \alpha)\left[aT_\infty + b\right] + \frac{W}{A} + \frac{hr'V^2}{2C_p}}{(1 - G)\,h - \sigma a(\epsilon - \alpha)}$$

For finite zero gain, $\beta = \frac{g}{g_o}$ the equilibrium error is

$$\Delta T_e = \frac{\left(T_{oe} + T_\infty\right)\left(Gh + \sigma\epsilon a + \frac{K}{A}\right) + (\beta + 1)\left[\sigma b(\epsilon - \alpha) + \frac{W}{A} + \frac{hr'V^2}{2C_p}\right] + \beta\sigma a(\epsilon - \alpha)\,T_\infty}{h + \sigma\delta a + \frac{K}{A} + \beta\left[(1 - G)h - \sigma a(\epsilon - \alpha)\right]}$$

Finally, one might represent the passive shield concept in which the shield temperature is not controlled, but whose temperature T_s is monitored for data correction purposes, by letting $g = 0$.

In addition to the determining parameters G and r' it is necessary to evaluate h under the conditions of the flow at the sensor inside the duct. It is possible that the ventilation speed V_f is reduced and a different degree of turbulence exists in the duct, each perhaps varying with angle of attack at the duct entrance, and each in turn influencing h at the sensor. Further study of the aerodynamics of specific duct configurations and of the concomitant shield heat transfer problem would further establish the feasibility of the active shield concept. System mathematical models such as the one above would also be useful in prescribing experiments.

GLOSSARY

A — Sensor effective convective surface area (may vary according to roughness).

A_r — Sensor effective radiative surface area.

A_s — Shield effective convective inner surface area.

a, a_s — $4T_a^3$, linearizing factor for T^4, T_s^4.

b, bs — $3T_a^4$, linearizing term for T^4, T_s^4.

C — Sensor thermal capacity per area A.

C_s — Shield thermal capacity.

C_p — Specific heat of air.

D — Denominator of system transfer function.

G — λS_t, a dimensionless measure of the heating effect of the shield on the air stream.

g — Open-loop gain of the shield temperature control servo, or the heat flow rate per degree temperature difference $(T_s - T)$.

g_o — Linearizing factor for heat-flow rate to the shield from the environment.

h — Sensor effective convective coefficient

h_s Shield (duct) effective convective coefficient.

K Sensor conductive coefficient, heat-flow rate to the sensor through its supporting structure per degree difference $\left(T - T_s\right)$.

L Characteristic length associated with the shield.

$\dot{m}$ Air mass rate through the duct.

r Sensor recovery factor.

r_s Shield (duct) recovery factor.

r' Over-all effective recovery factor, $r\left(\frac{V_f}{V}\right)^2 - Gr_s$.

S Laplace transform variable.

S_t Duct Stanton number, $\frac{Nu}{Re\,Pr} = \frac{h_s}{\rho V C_p}$.

T Sensor temperature.

T_a Nominal temperature for linearizing purposes.

T_e Equilibrium temperature of sensor.

T_f Recovery temperature at the sensor.

T_{oe} Equilibrium temperature of the shield with respect to its environment (excluding control system).

T_{rs} Recovery temperature of duct.

T_s Shield (duct) temperature.

T_∞ Atmospheric temperature.

T'_∞ Air stream temperature at the sensor

t Time.

V Free stream speed, sonde fall speed.

V_f Sensor ventilation air speed.

W Sensor electrical heating power.

α Sensor absorptivity (long wave).

β Nondimensional servo gain, g/g_o.

ϵ Duct emmissivity (long wave).

λ Nondimensional duct surface area, ratio of shield inner surface (preceding the sensor) to the effective duct aperture $\dot{m}/\rho V$.

Σ, Σ_s Net heat input rate (per area for Σ) to the sensor field.

σ Stefan-Boltzmann constant.

τ Sensor time constant.

τ_s Shield time constant.

REFERENCES

1. Billings, R. Gail, "Improving the Accuracy and Extending the Maximum Altitude of Mesospheric Temperature Measurements," paper delivered at the Amer. Meteor Soc/American Institute of Aeronautics and Astronautics Sixth Conference on Applied Meteorology, Los Angeles, 31 March, 1966.

2. Carley, C. T., Jr., and Smetana, S. O., "Experiments on Transition Regime Flow Through a Short Tube with a Bell Mouth Entry," Amer. Inst. of Aeron. and Astron. J., Vol. 4, January 1966, pp. 47-54.

3. Mason, Samuel J., "Feedback Theory -- Some Properties of Signal-Flow Graphs," Proc. IRE, Vol. 41, September 1953, pp. 1144-1156.

4. Mason, Samuel J., "Feedback Theory -- Further Properties of Signal Flow Graphs," Proc. IRE, Vol. 44, July 1956, pp. 920-926.

5. Kreith, Frank, Principles of Heat Transfer, International Textbook Company, Scranton, Pennsylvania, 1958, Chapter 8.

APPENDIX F

COMMENTS ON EVALUATION OF RADAR ERRORS FROM SPHERE-RADAR RECORDS

Inflated radar-tracked falling sphere meteorological experiments, especially those in which the sphere traverses an appreciable region after ejection, in which its motion is insensitive to the atmosphere, provide radar data consisting of the following phases: The first is the track of the vehicle (rocket) from the launcher to ejection of the sphere. This phase may be divided into thrust and coast portions. The second phase is the record of the ascending sphere until decreased speed and air density cause atmospheric drag to become insignificant. The third is the low-drag phase near apogee. The fourth phase occurs when the sphere is again sufficiently decelerated by drag to provide meteorological data. The fifth phase occurs when increased atmospheric pressure causes collapse of the sphere. Data subsequent to collapse is generally regarded as useless.

It appears that circumstances attending the radar target in the first phase (pre-ejection) and the low-drag phase (near-vacuum trajectory) permit the measurement of radar error parameters in those phases for the purpose of "per-flight" corrections of the data in the sensing phases. For the measurement of certain of the error parameters, the low-drag phase may prove to be most appropriate.

In the low-drag phase the sphere is essentially drag free so that the target motion may be expected to be very smooth, even in the presence of possible atmospheric inhomogeneities. Thus, a good approximation to

the real trajectory should be possible (especially when more than one radar has tracked the target) and a large class of excursions from this smooth approximation should be assignable to the measuring system. A careful analysis of these excursions will hopefully lead to identification and classification according to radar subsystems and to deriving parameter values appropriate to subsequent data correction and/or data evaluation. A valid systematic point-by-point estimation of the uncertainty in the meteorological data due to radar performance, as demonstrated in the first and third phases of the same tracking mission, would be of great benefit to users and developers alike. If in addition, however, it becomes possible to correct the data according to the measured radar performance, the payoff is even greater. The measurement of deterministic error parameters (repeating system nonlinearities) may allow data corrections. The remaining errors may be measurable in terms of random parameters and may provide bases for error estimates in the meteorological data.

The motion of the target in the low-drag phase is that of a point mass, since there exist no significant coupling mechanisms between rotational and translational motions of the sphere. (The radar generally is sensitive to sphere rotation through amplitude modulations of the radar return. Provision for this may be considered later.) The motion of a point mass is given, according to Newton's law, with respect to an inertial (nonaccelerating, nonrotating) frame of reference. The accelerating force is that of gravitational attraction to a distributed mass (the earth). If gravitational anomalies are small enough (or not known) with respect to a given sphere trajectory, the gravitational field

may be approximated by an appropriate central force field, which in turn suggests a coordinate system containing a radial member along which the accelerating force is directed.* Finally, the motion is observed in a rotating (earth-fixed) frame of reference, using spherical coordinates (radar range, elevation, azimuth) with origin displaced from the axis of the earth's rotation. Each radar coordinate is expected to exhibit its own error and noise characteristics, therefore it is desired ultimately to express the motion in terms of these coordinates.

An adequate mathematical model of the sphere trajectory may therefore involve at least three coordinate systems (or some variation of these):

1. A rectlinear inertial system in which the equations of motion are solved.
2. An earth-fixed system in which to define the gravitational acceleration and a drag perturbation factor, to locate the radar site, and perhaps to relate a missile range coordinate system already defined and used by local organizations.
3. A radar coordinate system which is also earth fixed but using the modified spherical coordinates of the radar with origin at the radar site.

In order to maximize the region of validity of the low-drag phase sphere model, it is suggested that the drag term be included but that it

---

* This in general will not be "down" to an observer on the earth since his "plumb bob" would be accelerated toward the earth's rotational axis through its mount by the centripetal force arising from the earth's rotation.

be viewed as a judiciously selected perturbation term. Buoyancy and wind effects are omitted by definition of the low-drag phase.

A smoothing process based on the model, that is, based on accurate knowledge of the signal (target motion), will enable the extraction of the signal from the data. The remainder, in terms of a noise function for each output channel of the radar, permits a close study of the noise based on detailed knowledge of potential noise sources in the various radar subsystems. Each of the three functions will be analyzed for correlations with hardware states and substates. Microwave propagation and interference effects will be considered. Statistical distributions and amplitudes will be investigated with and without discernable deterministic errors. Findings will determine the feasibility of a correction and/or data evaluation scheme, and will suggest succeeding action.